Synthetic Models for the Zinc Sites in the Methionine Synthases

Show-Jen Chiou, Julie Innocent, Charles G. Riordan,* Kin-Chung Lam, Louise Liable-Sands, and Arnold L. Rheingold

Department of Chemistry and Biochemistry, University of Delaware, Newark, Delaware 19716

Received May 11, 2000

The syntheses and molecular structures of a series of tetrahedral zinc complexes designed to model the active sites in *Escherichia coli* methionine synthases are reported. [PhTt$^{t\mathrm{Bu}}$]ZnBr (PhTt$^{t\mathrm{Bu}}$ = phenyltris((*tert*-butylthio)-methyl)borate) was prepared and characterized crystallographically to provide entry into [S_3]ZnX complexes. Metathesis with KSPh yielded the phenylthiolato complex, [PhTt$^{t\mathrm{Bu}}$]Zn(SPh), which represents a structural mimic of the homocysteine ligated form of the enzyme. Alternatively, [S_2N]ZnX (X = Br, CH_3, SPh) species were prepared using the new mixed-donor ligands, [Ph(pz)Bt$^{t\mathrm{Bu}}$] (phenyl(pyrazolyl)bis((*tert*-butylthio)methyl)borate) and [Ph(pz$^{t\mathrm{Bu}}$)Bt$^{t\mathrm{Bu}}$] (phenyl(3-*tert*-butylpyrazolyl)bis((*tert*-butylthio)methyl)borate). Protonolysis of [Ph(pz$^{t\mathrm{Bu}}$)-Bt$^{t\mathrm{Bu}}$]Zn(CH_3) by PhSH in toluene yielded [Ph(pz$^{t\mathrm{Bu}}$)Bt$^{t\mathrm{Bu}}$]Zn(SPh), a synthetic analogue of the homocysteine ligated form of cobalamin-independent methionine synthase (Met E). The average Zn−S bond distance in [Ph-(pz$^{t\mathrm{Bu}}$)Bt$^{t\mathrm{Bu}}$]Zn(SPh) of 2.37 Å compares well with the EXAFS-derived distance of 2.31 Å found in the homocysteine-bound form of Met E.

Introduction

Zinc is an essential metal ion in biological processes, playing a seminal role in the structure and function of a wide range of metalloproteins. Structural zinc sites include, for example, zinc finger proteins which regulate gene transcription and a structural ion in the enzyme liver alcohol dehydrogenase.[1] A common feature of structural zinc sites is tetrahedral coordination in which all four donors are protein residues. In this sense the metal ion is coordinatively saturated. Alternatively, when zinc has been sequestered for a catalytic function, an exogenous (and labile) donor such as water occupies one of the four coordination sites. Examples include mononuclear sites as in carbonic anhydrase (CA), liver alcohol dehydrogenase (LADH), and the methionine synthases.[2] In these proteins the zinc is coordinated by three side chain residues and an exogenous donor. Presumably, catalysis requires a labile coordination site to allow for substrate binding in a four-coordinate structure. However, this is far from certain given the propensity with which zinc can access higher coordination numbers. For example, the catalytic zinc in the endopeptidase astacin is five coordinate as deduced crystallographically.[3] While the common feature that three protein residues ligate zinc in many catalytic sites has emerged, the identity of these residues varies greatly. In general, the sites may be characterized as Zn[$N_xO_yS_z$] ($x + y + z = 3$ or 4). In CA, the three donors are histidines while in LADH the ligands are two cysteines and a histidine.[4] In farnesyl transferase all three donor atom types are present: histidine, cysteine, aspartate (bidentate), and a water molecule.[5] Despite the growing structural database of zinc proteins, the extent to which the nature of the protein ligands defines the diverse catalytic function remains unclear. Small molecule analogues would clearly aid in developing a deeper understanding of relevant zinc coordination chemistry with the goal of developing functional (catalytic) models.[6−11]

The de novo biosynthesis of the amino acid methionine from homocysteine (Hcys) requires methyl group transfer, a reaction catalyzed by the metalloenzyme methionine synthase.[2] The reaction involves CH_3−H_4folate as the one-carbon donor and Hcy as the acceptor, Scheme 1. Nature has evolved two pathways for this process. One, termed the cobalamin-dependent methionine synthase (Met H), involves the intermediacy of methylcobalamin. In this two-step process the methyl group is transferred first from CH_3−H_4folate to cob(I)alamin, Scheme 2. In a distinct step methylcobalamin alkylates Hcys yielding Met and regenerating cob(I)alamin. The other pathway does not employ the cobalamin cofactor. Instead the reaction proceeds by direct transmethylation from CH_3−H_4folate to Hcys (cobalamin-independent methionine synthase, Met E). Matthews has demonstrated recently that zinc is required for *both* enzymes.[12,13] Several elegant biophysical studies have been reported, resulting in proposals for the active site structures and function of the zinc ion.[14−16] In Met H, the zinc is ligated by three sulfur donors, presumably cysteines and/or methionines, and a nitrogen or

(1) Lipscomb, W. N.; Sträter, N. *Chem. Rev.* **1996**, *96*, 2375−2434.
(2) Matthews, R. G.; Goulding, C. W. *Curr. Opin. Chem. Biol.* **1997**, *1*, 332−339.
(3) Bode, W.; Gomis-Rueth, F. X.; Huber, R.; Zwilling, R.; Stoecker, W. *Nature* **1992**, *358*, 164−167.
(4) Benach, J.; Atrian, S.; Gonzalez-Duarte, R.; Ladenstein, R. *J. Mol. Biol.* **1998**, *282*, 383−399.
(5) Park, H.-W.; Boduluri, S. R.; Moomaw, J. F.; Casey, P. J.; Beese, L. S. *Science* **1997**, *275*, 1800−1804.
(6) Looney, A.; Han, R. V.; McNeill, K.; Parkin, G. *J. Am. Chem. Soc.* **1993**, *115*, 4690−4697.
(7) Bergquist, C.; Parkin, G. *J. Am. Chem. Soc.* **1999**, *121*, 6322−6323.
(8) Brand, U.; Rombach, M.; Vahrenkamp, H. *Chem. Commun.* **1998**, 2717−2718.
(9) Grapperhaus, C. A.; Tuntulani, T.; Reibenspies, J. H.; Darensbourg, M. Y. *Inorg. Chem.* **1998**, *37*, 4052−4058.
(10) Hammes, B. S.; Carrano, C. J. *Inorg. Chem.* **1999**, *38*, 4593−4600.
(11) Kimblin, C.; Hascall, T.; Parkin, G. *Inorg. Chem.* **1997**, *36*, 5680−5681.
(12) Gonzalez, J. C.; Peariso, K.; Penner-Hahn, J. E.; Matthews, R. G. *Biochemistry* **1996**, *35*, 12228−12234.
(13) Goulding, C. W.; Matthews, R. G. *Biochemistry* **1997**, *36*, 15749−15757.
(14) Gonzalez, J. C.; Goulding, C. W.; Jarrett, J.; Peariso, K.; Penner-Hahn, J. E.; Matthews, R. G. *Protein Eng.* **1997**, 57.

10.1021/ic000505q CCC: $19.00
Published on Web 08/26/2000

Scheme 1

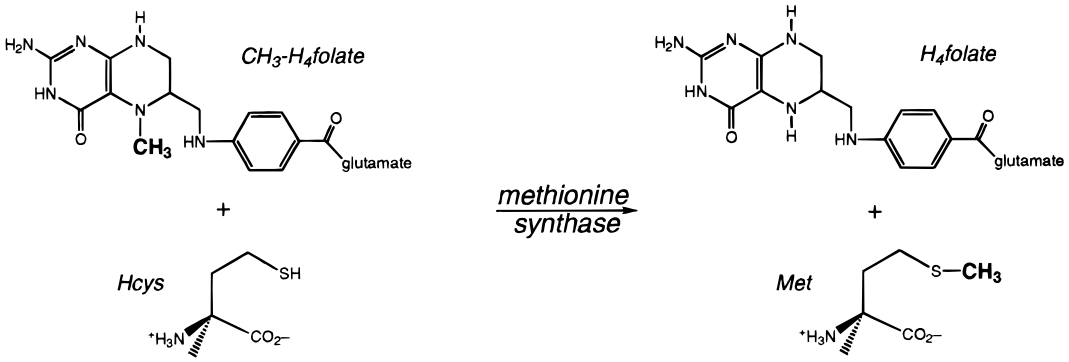

Scheme 2

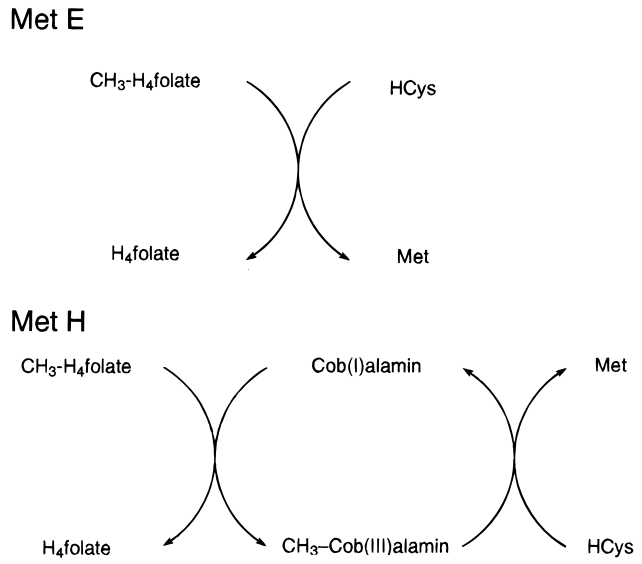

oxygen ligand, in a four-coordinate structure. Upon incubation with Hcy the N/O donor is replaced by homocysteine yielding an all-sulfur environment. In Met E, the zinc is initially in a $[S_2(N/O)_2]$ environment that changes to $[S_3(N/O)_1]$ when the enzyme is exposed to Hcy. The changes for each enzyme have been interpreted to indicate that homocysteine binds to zinc displacing the light atom (N or O) ligand.[15] Metal binding presumably activates homocysteine for transmethylation by rendering it ionized (as the thiolate) at neutral pH; thiolate anions are more nucleophilic than neutral thiols. However, it is not known to what degree a thiolate's nucleophilicity is modulated by coordination to a metal ion. Recent work by our group[17] and others[9,18] has begun to quantify this effect.

This paper details our initial efforts to develop a better understanding of the reaction pathway of the methionine synthases, specifically the ability of zinc to activate homocysteine for attack by electrophiles, through the study of synthetic model complexes. As shown in Scheme 3, the borato ligands developed in our laboratories are ideally suited for this pursuit.[19−21] They provide the necessary ancillary ligand framework—face-capping array of donor groups— to permit investigation *and* comparison of the zinc sites in both Met H and Met E. Contained herein is the preparation of the necessary ligands and their zinc derivatives, including monomeric zinc thiolates, that serve as models for the Hcy-bound forms of the methionine synthases. Outcomes from these studies have broad implications to a wide range of zinc protein catalyzed transalkylations to thiols including methyl reductase,[22] the Ada protein,[23] farnesyl transferase,[5] betaine homocysteine methyltransferase,[24] and epoxyalkane coenzyme M transferase.[25] Consequently, we aim to bring our understanding of thiol activating zinc proteins in line with the much more established roles of zinc in maintaining structural integrity and catalyzing hydrolysis reactions.

Results

Ligand Syntheses. The preparation of the mixed-donor $[NS_2]$ ligands, $[Ph(pz)Bt^{tBu}]H$ and $[Ph(pz^{tBu})Bt^{tBu}]H$, proceeds smoothly employing a one-pot, stepwise protocol.[26] Using $PhBCl_2$ as the borane source, the *tert*-butyl thioether substituents were introduced first by addition of 2 equiv of $LiCH_2S^tBu$. Then the appropriate pyrazolate was added as its Li^+ salt. Aqueous workup yielded gram quantities of the "free acid" ligand. The compounds are white, crystalline solids stable in air and soluble in a range of organic solvents. Their ^1H NMR spectra exhibit clearly resolved resonances for the pyrazolyl and phenyl hydrogens. Most characteristic are the downfield resonance for the "acid" proton at δ 13.5 and the diastereotopic methylene protons that appear as doublets at δ 2.2−2.0. The "free acid" form of the ligands proved suitable for the direct addition to organozinc precursors.

Preparation of Metal Complexes. The synthesis of the tetrahedral zinc complexes is outlined in Scheme 3. The $[PhTt^{tBu}]$ derivatives were accessed using $ZnBr_2$ as starting material. Addition of $[PhTt^{tBu}]Tl$[20] to anhydrous $ZnBr_2$ in diethyl ether produced $[PhTt^{tBu}]ZnBr$. The ^1H NMR spectrum of $[PhTt^{tBu}]ZnBr$ contains single resonances for the methylene and

(15) Pearlso, K.; Goulding, C. W.; Huang, S.; Matthews, R. G.; Penner-Hahn, J. E. *J. Am. Chem. Soc.* **1998**, *120*, 8410−8416.
(16) Zhou, Z. S.; Pearlso, K.; Penner-Hahn, J. E.; Matthews, R. G. *Biochemistry* **1999**, *38*, 15915−15926.
(17) Ram, M. S.; Riordan, C. G.; Ostrander, R.; Rheingold, A. L. *Inorg. Chem.* **1995**, *34*, 5884−5892.
(18) Wilker, J. J.; Lippard, S. J. *Inorg. Chem.* **1997**, *36*, 969−978.
(19) Ge, P.; Riordan, C. G.; Haggerty, B. S.; Rheingold, A. L. *J. Am. Chem. Soc.* **1994**, *116*, 8406−8407.
(20) Schebler, P.; Riordan, C. G.; Guzei, I.; Rheingold, A. L. *Inorg. Chem.* **1998**, *37*, 4754−4755.
(21) Chiou, S.; Ge, P.; Liable-Sands, L. M.; Rheingold, A. L. *Chem. Commun.* **1999**, 159−160.
(22) Ermler, U.; Grabarse, W.; Shima, S.; Goubeaud, M.; Thauer, R. K. *Science* **1997**, *278*, 1457−1462.
(23) Myers, L. C.; Terranova, M. P.; Ferentz, A. E.; Wagner, G.; Verdine, G. L. *Science* **1993**, *261*, 1164−1167.
(24) Breksa, A. P., III; Garrow, T. A. *Biochemistry* **1999**, *38*, 13991−13998.
(25) Allen, J. R.; Clark, D. D.; Krum, J. G.; Ensign, S. A. *Proc. Natl. Acad. Sci. U.S.A.* **1999**, *96*, 8432−8437.
(26) $PhTt^{tBu}$, phenyltris((*tert*-butylthio)methyl)borate; $[Ph(pz)Bt^{tBu}]$, phenyl(pyrazolyl)bis((*tert*-butylthio)methyl)borate; $[Ph(pz^{tBu})Bt^{tBu}]$, phenyl(3-*tert*-butylpyrazolyl)bis((*tert*-butylthio)methyl)borate.

Scheme 3

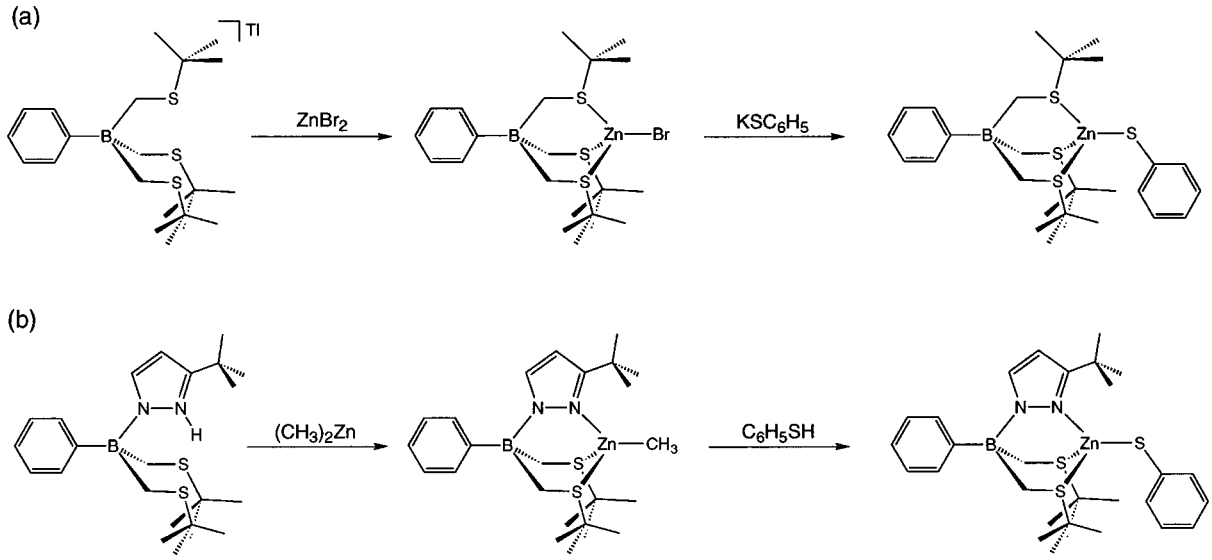

tert-butyl protons consistent with C_3-symmetric binding of the borato ligand. The molecular structure of [PhTt$^{t\mathrm{Bu}}$]ZnBr, as determined by X-ray diffraction, is described below. An analogous reaction between [PhTt$^{t\mathrm{Bu}}$]Tl and $CdCl_2$ yielded dimeric {[PhTt$^{t\mathrm{Bu}}$]CdCl}$_2$. Synthesis of a monomeric zinc thiolate was achieved by metathetical replacement of bromide in [PhTt$^{t\mathrm{Bu}}$]ZnBr with phenylthiolate. [PhTt$^{t\mathrm{Bu}}$]Zn(SPh) is highly soluble in low-polarity solvents including pentanes and diethyl ether.

Zinc complexes of the [NS_2] ligand [Ph(pz)Bt$^{t\mathrm{Bu}}$] were prepared in a similar fashion. [Ph(pz)Bt$^{t\mathrm{Bu}}$]Na was generated *in situ* via the addition of [Ph(pz)Bt$^{t\mathrm{Bu}}$]H to NaH in THF. Subsequent addition of 1 equiv of $ZnBr_2$ yielded [Ph(pz)Bt$^{t\mathrm{Bu}}$]ZnBr. The ^{1}H NMR spectrum of [Ph(pz)Bt$^{t\mathrm{Bu}}$]ZnBr exhibits resonances within *ca.* 0.1 ppm of those for the "free acid" ligand, absent the acid proton resonance. Again, the methylene hydrogens appear as two second-order doublets, a consequence of their diastereotopic relationship. Reaction of [Ph(pz)Bt$^{t\mathrm{Bu}}$]ZnBr with KSPh leads to production of [Ph(pz)Bt$^{t\mathrm{Bu}}$]Zn(SPh). However, this complex is unstable in solution. Over a period of days it decomposed to a mixture of products that included $[Zn(SPh)_4]^{2-}$.[27] The generation of the disproportionation product indicated that this route would not be satisfactory for the preparation of [Ph(pz)Bt$^{t\mathrm{Bu}}$]Zn(SPh). Consequently, all subsequent transformations utilizing [NS_2] borato ligands focused on the sterically more demanding ligand, [Ph(pz$^{t\mathrm{Bu}}$)Bt$^{t\mathrm{Bu}}$]. The additional *tert*-butyl substituent on the pyrazolyl ring was designed to provide sufficient steric bulk so as to preclude disproportionation reactions leading to [Ph(pz$^{t\mathrm{Bu}}$)Bt$^{t\mathrm{Bu}}$]$_2$Zn and $[Zn(SPh)_4]^{2-}$. As detailed below, this design works as intended.

Reaction of [Ph(pz$^{t\mathrm{Bu}}$)Bt$^{t\mathrm{Bu}}$]H with $(CH_3)_2Zn$ led to clean formation of [Ph(pz$^{t\mathrm{Bu}}$)Bt$^{t\mathrm{Bu}}$]Zn(CH_3) and methane, Scheme 3. In contrast to the spectra of the "free acid" ligands and their metal complexes, the ^{1}H NMR spectrum of [Ph(pz$^{t\mathrm{Bu}}$)Bt$^{t\mathrm{Bu}}$]Zn(CH_3) displayed a single, sharp resonance for the methylene hydrogens. This observation is interpreted as coincident degeneracy of the diastereotopic proton resonances. The remaining signals for [Ph(pz$^{t\mathrm{Bu}}$)Bt$^{t\mathrm{Bu}}$]Zn(CH_3) are unexceptional including the zinc-bound methyl protons, δ −0.27. Low-temperature protonolysis of [Ph(pz$^{t\mathrm{Bu}}$)Bt$^{t\mathrm{Bu}}$]Zn(CH_3) with PhSH yielded [Ph(pz$^{t\mathrm{Bu}}$)Bt$^{t\mathrm{Bu}}$]Zn(SPh) as a white crystalline solid. This compound was characterized by ^{1}H NMR spectroscopy and X-ray diffraction. Unlike the less hindered [Ph(pz)Bt$^{t\mathrm{Bu}}$]Zn(SPh), this material is quite robust, showing no evidence of disproportionation.

Molecular Structures. The solid-state structures of [PhTt$^{t\mathrm{Bu}}$]ZnBr, {[PhTt$^{t\mathrm{Bu}}$]CdCl}$_2$, and [Ph(pz)Bt$^{t\mathrm{Bu}}$]ZnBr have been elucidated by X-ray diffraction. Molecular structures, presented as thermal ellipsoid plots, are contained in Figure 1. Selected metric parameters are contained in Table 2. [PhTt$^{t\mathrm{Bu}}$]ZnBr is isostructural with the previously reported [PhTt$^{t\mathrm{Bu}}$]NiCl and [PhTt$^{t\mathrm{Bu}}$]CoCl.[20] This complex is a rare example of a four-coordinate zinc thioether species that has been structurally authenticated. The face-capping ligand provides three thioether donors with an average Zn−S bond length of 2.360 Å. This distance compares favorably to the EXAFS-derived distance of 2.31 Å for the three sulfur ligands in Met H. Each of the three *tert*-butyl groups is canted in the same direction to minimize van der Waals contacts. The resulting pocket at the metal ion is rather shallow due to this canting. The Br completes the approximate tetrahedral zinc geometry residing within the cavity with Zn−Br of 2.310(1) Å.

{[PhTt$^{t\mathrm{Bu}}$]CdCl}$_2$ crystallized as a dimer with bridging chloride ligands, Figure 1B. The molecule resides on a crystallographically imposed inversion center rendering the metal ligation spheres metrically equivalent. The Cd coordination geometry is trigonal bipyramidal. One sulfur (S3 or S3A) and one chloride occupy the axial positions with the remaining sulfurs and chloride equatorial. Expectedly, the S3−Cd−Cl1A angle is nearly linear, 174.54(1)°. The equatorial Cd−S distances of 2.580(1) and 2.592(1) Å are shorter than the axial Cd−S distance, 2.730(1) Å. This molecule is only the second five-coordinate Cd thioether complex to be characterized crystallographically.[28]

The molecular structure of [Ph(pz)Bt$^{t\mathrm{Bu}}$]ZnBr is contained in Figure 1C. The [NS_2] borato ligand provides one nitrogen and two sulfur donors in a facial arrangement. The Zn−S distances, 2.374(1) and 2.402(1) Å, are longer slightly than those found in [PhTt$^{t\mathrm{Bu}}$]ZnBr. The Zn−N distance, 2.002(1) Å, is consistent with bond lengths reported for Tp$^{\mathrm{R}}$ZnX complexes.[6,7] In comparison, the bond distances for the zinc site in Met E

(27) Holah, D. G.; Coucouvanis, D. *J. Am. Chem. Soc.* **1975**, *97*, 6917−6919.

(28) Griffith, E. A. H.; Charles, N. G.; Rodesiler, P. F.; Amma, E. L. *Polyhedron* **1985**, *4*, 615−620.

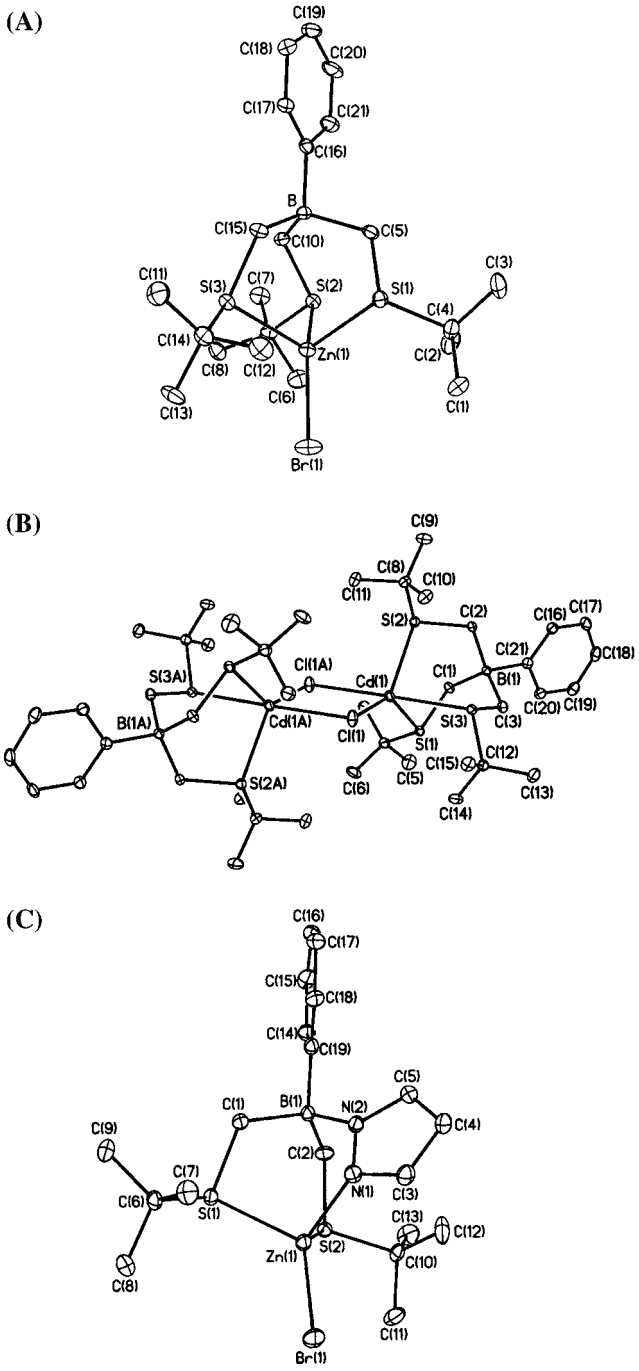

Figure 1. Thermal ellipsoid plots of (A) [PhTt^{tBu}]ZnBr, (B) {[PhTt^{tBu}]-CdCl}$_2$, and (C) [Ph(pz)Bt^{tBu}]ZnBr. Thermal ellipsoids are drawn at the 30% probability level, and hydrogen atoms are omitted for clarity.

are Zn−S, 2.31 Å, and Zn−N, 2.03 Å.[15] Similar distances are found for the catalytic site in LADH in which zinc is coordinated by two cysteines, one histidine, and an exogenous water ligand.[29] The S−Zn−S bite angle of 86.91(2)° is significantly smaller than the S−Zn−N bite angles of 102.85(6) and 100.63(6)°. The smaller S−Zn−S angle may be a consequence of an unusual feature of the structure. That is, the two *tert*-butyl groups are canted in *opposite* directions. When the structure is viewed down the Zn−Br vector, one *tert*-butylthio group is seen to be rotated clockwise while the other is rotated counterclockwise. This conformation greatly minimizes van der Waals contacts between these *tert*-butyl sulfur substituents. Presumably, the minimal steric requirements of the planar pyrazolyl group favor this conformation.

The structure of monomeric [Ph(pz^{tBu})Bt^{tBu}]Zn(SPh) is depicted in Figure 2 with selected metric parameters contained in Table 2. The [NS$_3$] coordination sphere includes two thioether and one pyrazolyl donor provided by the borato ligand and the phenylthiolato group in a distorted tetrahedral geometry. Given the proclivity with which thiolates occupy bridging positions, the monomeric structure is undoubtedly a consequence of the steric protection provided by the three *tert*-butyl substituents of [Ph(pz^{tBu})Bt^{tBu}]. The average thioether Zn−S bond length, 2.43 Å, is longer than the thiolato Zn−S, 2.265(1) Å. The thioether distances are also slightly longer than those found in [Ph(pz)Bt^{tBu}]ZnBr. The average of the three Zn−S bond distances, 2.37 Å, is strikingly close to that in the Hcy bound form of Met E, 2.31 Å, as determined by EXAFS.[9] However, the Zn−N distance is essentially unchanged at 2.033(3) Å. Again the two *tert*-butyl groups on the S donors are canted in opposite directions, resulting in a small S1−Zn−S2 angle of 86.01(4)°. The thiolato ligand is bent away from the *tert*-butyl pyrazolyl group as evidenced by the large S3−Zn−N angle of 126.4(1)°. The phenyl substituent of this ligand is on the opposite side of the Zn−S3 vector from the pyrazole, placing it in a position where it essentially bisects the S1−Zn−S2 angle; N1−Zn−S3−C29 dihedral angle, 171.9°. This conformation minimizes interaction between the 3-*tert*-butylpyrazolyl substituent and the phenyl thiolate.

Discussion

To date most efforts in modeling catalytic zinc sites have focused on CA and LADH. These endeavors have commonly utilized tripodal ligands that provide nitrogen donors to mimic the native protein residues. Given that many of the catalytic sites contain a mixture of donor types, we have chosen to pursue face-capping ligands that contain donors that more faithfully model the protein residues. In the present study this requires either a [S$_3$] ligand for Met H or an [NS$_2$] ligand for Met E. Our tris((alkylthio)methyl)borato ligands have proven successful for the former target.[19,20] For the latter, recently we developed a mixed-donor ligand containing one nitrogen and two sulfur substituents.[21] Related mixed-donor ligands for modeling zinc enzymes have been reported by Parkin,[11,30] Vahrenkamp,[31] and Carrano.[10] As delineated below, our ligands are distinct and provide certain advantages we seek to exploit.

The borato ligands provide multiple thioether donors to the metal. The choice of thioether donors vs thiolate donors allows for greater control or "tunability" of the ligand's steric and electronic properties. The thioether substituent may be systematically varied to impart the desired properties at the metal center. In the present case, the *tert*-butyl groups prevent the formation of octahedral [PhTt^{tBu}]$_2$Zn, thereby allowing for [PhTt^{tBu}]ZnX complex formation. In the Tp^R ligands substituent changes are most commonly employed at the 3-pyrazole position to direct steric control. As this position is on the carbon adjacent to the donor nitrogen, the electronic changes provided are somewhat attenuated. However, in the [PhTt^R] ligands substituent changes have a greater impact on the electronic properties of the ligand as these groups are bound *directly* to the donor sulfur. Furthermore, the thioether donors have a greatly reduced propensity to bridge metals compared to thiolate ligands.

(29) Ramaswamy, S.; Eklund, H.; Plapp, B. V. *Biochemistry* **1994**, *33*, 5230−5237.
(30) Ghosh, P.; Parkin, G. *Chem. Commun.* **1998**, 413−414.
(31) Brand, U.; Vahrenkamp, H. *Inorg. Chem.* **1995**, *34*, 3285−3293.

Table 1. Crystallographic Data for [PhTt$^{t\mathrm{Bu}}$]ZnBr, {[Ph(pz)Bt$^{t\mathrm{Bu}}$]CdCl}$_2$, [Ph(pz)Bt$^{t\mathrm{Bu}}$]ZnBr and [Ph(pz$^{t\mathrm{Bu}}$)Bt$^{t\mathrm{Bu}}$]Zn(SPh)

	[PhTt$^{t\mathrm{Bu}}$]ZnBr	{[Ph(pz)Bt$^{t\mathrm{Bu}}$]CdCl}$_2$	[Ph(pz)Bt$^{t\mathrm{Bu}}$]ZnBr	[Ph(pz$^{t\mathrm{Bu}}$)Bt$^{t\mathrm{Bu}}$]Zn(SPh)
formula	$C_{21}H_{38}BBrS_3Zn$	$C_{44}H_{80}B_2Cd_2Cl_6S_6$	$C_{19}H_{30}BBrN_2S_2Zn$	$C_{29}H_{43}BN_2S_3Zn$
fw	542.78	1260.56	506.66	592.01
space group	$P2_1/n$	$P\bar{1}$	$P\bar{1}$	*Pbca*
a, Å	9.74863(2)	9.6736(2)	9.8538(2)	15.6479(2)
b, Å	21.2707(3)	12.3338(2)	9.9162(2)	18.0911(2)
c, Å	12.7166(2)	13.7419(2)	12.0741(2)	22.4118(2)
α, deg	90.00	65.2684(4)	95.4226(2)	90.00
β, deg	98.7525(7)	77.4098(4)	93.2470(2)	90.00
γ, deg	90.00	77.2047(2)	100.1906(8)	90.00
V, Å^3	2606.20(7)	1437.60(2)	1152.74(3)	6344.4(1)
Z	4	1	2	8
cryst color, habit	colorless rod	colorless plate	colorless block	colorless plate
D(calc), g cm^{-3}	1.383	1.456	1.460	1.240
μ(Mo Kα), cm^{-1}	27.21	12.65	29.86	9.91
temp, K	173(2)	173(2)	173(2)	213(2)
diffractometer			Siemens P4/CCD	
radiation			Mo Kα (λ = 0.71073 Å)	
$R(F)$, %[a]	4.38	2.58	3.13	6.65
$R(wF^2)$, %[a]	10.03	11.14	13.92	11.56

[a] Quantity minimized = $R(wF^2) = \sum[w(F_o^2 - F_c^2)^2]/\sum[(wF_o^2)^2]^{1/2}$; $R = \sum\Delta/\sum(F_o)$, $\Delta = |(F_o - F_c)|$, $w = 1/[\sigma^2(F_o^2) + (aP)^2 + bP]$, $P = [2F_c^2 + \mathrm{Max}(F_o,0)]/3$.

Table 2. Selected Bond Lengths (Å) and Bond Angles (deg) for [PhTt$^{t\mathrm{Bu}}$]ZnBr, {[Ph(pz)Bt$^{t\mathrm{Bu}}$]CdCl}$_2$, [Ph(pz)Bt$^{t\mathrm{Bu}}$]ZnBr, and [Ph(pz$^{t\mathrm{Bu}}$)Bt$^{t\mathrm{Bu}}$]Zn(SPh)

	[PhTt$^{t\mathrm{Bu}}$]ZnBr		
Zn−Br	2.3105(6)	Br−Zn−S2	118.87(3)
Zn−S1	2.3577(9)	S1−Zn−S2	97.65(3)
Zn−S2	2.3605(9)	Br−Zn−S3	119.80(3)
Zn−S3	2.3624(9)	S1−Zn−S3	96.90(3)
Br−Zn−S1	120.12(3)	S2−Zn−S3	98.56(3)
	{[Ph(pz)Bt$^{t\mathrm{Bu}}$]CdCl}$_2$		
Cd1−S1	2.5919(5)	Cl1−Cd1−Cl1	82.71(2)
Cd1−S2	2.5802(5)	S2−Cd1−Cl	94.77(2)
Cd1−S3	2.7299(5)	S1−Cd1−Cl	100.55(2)
Cd1−Cl1	2.5053(5)	Cl1−Cd1−S3	91.92(1)
Cd1−Cl1A	2.6870(5)	S2−Cd1−S3	87.57(1)
Cl1−Cd1−S2	126.38(2)	S1−Cd1−S3	84.12(1)
Cl1−Cd1−S1	138.21(2)	Cl1−Cd1−S3	174.54(2)
S2−Cd1−S1	95.08(2)		
	[Ph(pz)Bt$^{t\mathrm{Bu}}$]ZnBr		
Zn−Br	2.3215(3)	N1−Zn−S1	102.85(6)
Zn−N1	2.002(2)	Br−Zn−S1	123.58(2)
Zn−S1	2.3743(6)	N1−Zn−S2	100.63(6)
Zn−S2	2.4022(6)	Br−Zn−S2	122.61(2)
N1−Zn−Br	114.90(6)	S1−Zn−S2	86.91(2)
	[Ph(pz$^{t\mathrm{Bu}}$)Bt$^{t\mathrm{Bu}}$]Zn(SPh)		
Zn−S1	2.418(1)	N1−Zn−S1	101.7(1)
Zn−S2	2.441(1)	S3−Zn−S1	118.99(5)
Zn−S3	2.265(1)	N1−Zn−S2	98.4(1)
Zn−N1	2.033(3)	S3−Zn−S2	116.52(5)
N−Zn−S3	126.42(1)	S1−Zn−S2	86.01(4)

Consequently, the ability to control nuclearity outside of a protein matrix is enhanced by using thioether ligands. Finally, while cysteine thiolates are the most prevalent sulfur ligands in proteins, they are often stabilized by hydrogen bonding, Figure 3. This interaction serves to reduce the nucleophilicity of the cysteine, to dissipate charge buildup and to modulate redox properties in cases where cysteines are coordinated to redox active metal ions. *We contend that these properties are accurately mimicked with thioether donors in aprotic solvents.*

The discrete, monomeric thiolates, [PhTt$^{t\mathrm{Bu}}$]Zn(SPh) and [Ph(pz$^{t\mathrm{Bu}}$)Bt$^{t\mathrm{Bu}}$]Zn(SPh), represent the most accurate small molecule analogs to date of the zinc active sites in the methionine synthases. This is because the borato ligands provide appropriate coordination spheres, replicating the ligand atoms provided by the protein. [PhTt$^{t\mathrm{Bu}}$], coordinating through three thioethers, mimics the three sulfur donors in Met H. The ligand [Ph(pz$^{t\mathrm{Bu}}$)-

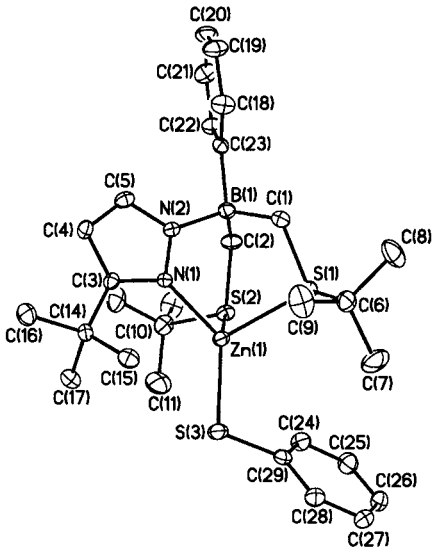

Figure 2. Thermal ellipsoid plot of [Ph(pz$^{t\mathrm{Bu}}$)Bt$^{t\mathrm{Bu}}$]Zn(SPh). Thermal ellipsoids are drawn at the 30% probability level, and hydrogen atoms are omitted for clarity.

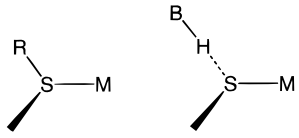

Figure 3. Comparison of coordinated thioether and coordinated thiolate that also participates in hydrogen bonding.

Bt$^{t\mathrm{Bu}}$] presents the [NS_2] coordination environment found in the cobalamin-independent Met E. In each of these complexes, the fourth ligand is phenylthiolate. As such it serves to represent homocysteine coordination to the zinc. Homocysteine coordination to zinc has been proposed to serve as an activating mechanism rendering the thiol highly acidic at physiological pH.[2] That is, coordination results in deprotonation making the homocysteine sufficiently nucleophilic to be alkylated. At present it is not well understood to what extent metal coordination reduces the nucleophilicity. Lippard and Wilker demonstrated that $[Zn(SPh)_4]^{2-}$ is alkylated by phosphotriesters via a dissociative pathway.[18,32] Their kinetic analysis is consistent with

the active species being "free thiolate". In other words, dissociated SPh^- is at least 2 orders of magnitude more reactive than the zinc-bound thiolate in $[Zn(SPh)_4]^{2-}$. Alternatively, we showed through kinetic studies that $[Ni(tmc)SPh]^+$ reacts with alkyl halides in a bimolecular mechanism in which the nickel-bound thiolate is alkylated.[17] In the latter case, "free thiolate" reacts more rapidly than bound thiolate, but the dissociation equilibrium lies in favor of coordinated SPh^-.

Summary and Prospectus

This report presents synthetic strategies to access several zinc complexes including two monomeric zinc thiolates, [PhTt$^{t\mathrm{Bu}}$]Zn(SPh) and [Ph(pz$^{t\mathrm{Bu}}$)Bt$^{t\mathrm{Bu}}$]Zn(SPh). These complexes represent the most accurate structural models to date for the active sites of Met E and Met H in the homocysteine-bound form of the proteins. Additionally, we include preliminary synthetic success in the preparation of a related cadmium halide that serves as a necessary precursor for entry into monomeric cadmium thiolates. Production of the chloride-bridged dimer, {[PhTt$^{t\mathrm{Bu}}$]CdCl}$_2$, highlights the differences between Zn and Cd coordination preferences, most notably, the greater ease with which Cd forms five-coordinate complexes. These differences are clearly significant in the context of activity of cadmium-substituted zinc proteins. For example, cadmium-substituted Met E is completely inactive.[2] In contrast, when the zinc in the DNA repair Ada protein is replaced by cadmium, activity is maintained.[23] Our current goals are directed toward the preparation of monomeric Cd thiolates and the alkylation of [PhTt$^{t\mathrm{Bu}}$]Zn(SPh) and [Ph(pz$^{t\mathrm{Bu}}$)Bt$^{t\mathrm{Bu}}$]Zn(SPh) with biologically relevant carbon electrophiles.

Experimental Section

Materials and Methods. All reagents were purchased from commercial sources and used as received, unless otherwise noted. Solvents were distilled under N_2 and dried as indicated. Toluene, hexanes, and diethyl ether were freshly distilled over Na/benzophenone. TMEDA was distilled over 3 Å molecular sieves under reduced pressure. *tert*-Butyl methyl sulfide[33] and 3-*tert*-butylpyrazole[34] were prepared as described previously. Manipulations involving organometallic reagents were performed under a nitrogen atmosphere either on a Schlenk line or in a Vacuum Atmospheres glovebox. Elemental analyses were performed by Desert Analytics, Inc., Tuscon, AZ. NMR spectra were recorded on a 250 MHz Brüker spectrometer.

CAUTION. *Dimethyl sulfide and tert-butyl mercaptan are flammable liquids that present a pungent odor. The deprotonation reaction should be vented through an aqueous solution of NaOCl and NaOH.*

[PhTt$^{t\mathrm{Bu}}$]ZnBr. [PhTt$^{t\mathrm{Bu}}$]Tl[20] (500 mg, 0.83 mmol) in 10 mL of CH_2Cl_2 was added to $ZnBr_2$ (187 mg, 0.83 mmol) in 15 mL of Et_2O, yielding a clear solution and white solid. The solution was stirred for 1 h. After filtration the solvent was removed under reduced pressure, yielding an off-white solid. The product was washed with Et_2O (2 × 10 mL). The resulting white solid was purified by recrystallization from CH_2Cl_2/Et_2O. Yield: 310 mg (68%). ^{1}H NMR ($CDCl_3$): δ 7.37 (d, *o*-C_6H_5, 2 H), 7.20 (t, *m*-C_6H_5, 2 H), 7.10 (t, *p*-C_6H_5, 1 H), 2.23 (br, BCH_2, 6 H), 1.45 (s, C(CH_3)$_3$, 27 H). Anal. Calcd (found) for $C_{21}H_{38}BBrS_3Zn$: C, 46.5 (46.1); H, 7.06 (6.98).

[PhTt$^{t\mathrm{Bu}}$]Zn(SPh). [PhTt$^{t\mathrm{Bu}}$]ZnBr (120 mg, 0.22 mmol) in 5 mL of THF was added to KSPh (33 mg, 0.22 mmol) in 5 mL of THF, yielding a clear solution. After 12 h, the white precipitate that formed was removed by filtration. The solvent was removed under reduced pressure, yielding a white solid. Yield: 92 mg (73%). ^{1}H NMR (CD_3CN): δ 7.51 (d, 4 H), 7.40 (br, 1 H), 6.93 (t, 1 H), 6.85 (t, 3 H), 6.75 (t, 1 H), 1.83 (q, BCH_2, 6 H), 1.20 (s, C(CH_3)$_3$, 27 H).

[Ph(pz)Bt$^{t\mathrm{Bu}}$]H. CH_3S^tBu (12 mL, 90 mmol) and TMEDA (2 mL) were placed in a 300 mL flask that was vented through an aqueous solution of NaOCl. BuLi (36 mL, 2.5 M in hexanes) was added dropwise via syringe over 5 min. After 4 h the solution was cooled to −78 °C and 40 mL of THF added. The resulting solution was cooled to −78 °C and added dropwise over 40 min to $PhBCl_2$ (6.1 mL, 45 mmol) in 100 mL of THF. The mixture was allowed to warm to 25 °C and stirred for an additional 30 min. Lithium pyrazolate, prepared *in situ* from pyrazole (3.1 g, 45 mmol) and BuLi (18 mL, 2.5 M in hexanes), was added to the borane solution at −78 °C. After stirring for 1 h the reaction was quenched by addition of 100 mL of H_2O. Volatile organics were removed under reduced pressure. The resulting yellow semisolid was dissolved in CH_2Cl_2 and dried over $CaCl_2$. The white product was precipitated from a concentrated solution of CH_2Cl_2 by addition of pentanes. Yield: 5.7 g (35%). [Ph(pz)Bt$^{t\mathrm{Bu}}$]H is soluble in THF, acetone, chlorinated hydrocarbons, methanol, and pentane. ^{1}H NMR ($CDCl_3$): δ 13.75 (s, N*H*, 1 H), 7.94 (d, 5-pz, 1 H), 7.67 (d, 3-pz, 1 H), 7.14 ((*o*-C_6H_5)B and (*p*-C_6H_5)B, m, 3 H), 6.93 (t, (*m*-C_6H_5)B, 2 H), 6.52 (t, 4-pz, 1 H), 2.23 (d, BCH_2, 2 H), 2.04 (d, BCH_2, 2 H), 1.27 (s, C(CH_3)$_3$, 18 H). Anal. Calcd (found) for $C_{19}H_{31}BN_2S_2$: C, 63.0 (62.6); H, 8.62 (8.66); N, 7.73 (7.75).

[Ph(pz$^{t\mathrm{Bu}}$)Bt$^{t\mathrm{Bu}}$]H. The free acid ligand was prepared in a manner analogous to that used for H[Ph(pz)Bt$^{t\mathrm{Bu}}$], with 3-*tert*-butylpyrazole used in place of pyrazole. The solubility of [Ph(pz$^{t\mathrm{Bu}}$)Bt$^{t\mathrm{Bu}}$]H in pentanes is greater than that of H[Ph(pz)Bt$^{t\mathrm{Bu}}$]. Additionally, the free acid is soluble in THF, acetone, methanol, and chlorinated hydrocarbons. Yield: 5.9 g (31%). ^{1}H NMR ($CDCl_3$): δ 13.58 (s, N*H*, 1 H), 7.73 (d, 5-pz, 1 H), 7.16 ((*o*-C_6H_5)B and (*p*-C_6H_5)B, m, 3 H), 6.92 (t, (*m*-C_6H_5)B, 2 H), 6.23 (t, 4-pz, 1 H), 2.24 (d, BCH_2, 2 H), 2.05 (d, BCH_2, 2 H), 1.37 (s, 3-C(CH_3)$_3$-pz, 9 H), 1.28 (s, C(CH_3)$_3$, 18 H). Anal. Calcd (found) for $C_{23}H_{39}BN_2S_2$: C, 66.0 (66.3); H, 9.39 (9.40); N, 6.69 (6.86).

[Ph(pz)Bt$^{t\mathrm{Bu}}$]ZnBr. [Ph(pz)Bt$^{t\mathrm{Bu}}$]H (3.62 g, 10 mmol) was deprotonated using NaH (0.24 g, 10 mmol) suspended in THF to form [Ph(pz)Bt$^{t\mathrm{Bu}}$]Na. [Ph(pz)Bt$^{t\mathrm{Bu}}$]Na (115 mg, 0.3 mmol) in 5 mL of CH_2Cl_2 was added to $ZnBr_2$ (67.5 mg, 0.3 mmol) in 15 mL of CH_2Cl_2/Et_2O, yielding a clear solution and white solid. After 1 h the solution was filtered and the solvent removed under reduced pressure. The resulting white solid was purified by recrystallization from CH_2Cl_2/Et_2O. Yield: 116 mg (77%). ^{1}H NMR ($CDCl_3$): δ 7.69 (d, 5-pz, 1 H), 7.42 ((*o*-C_6H_5)B, s, 2 H), 7.32 ((*p*-C_6H_5)B and (*m*-C_6H_5)B, m, 3 H), 7.10 (d, 3-pz, 1 H), 6.17 (t, 4-pz, 1 H), 2.20 (d, BCH_2, 2 H), 2.37 (d, BCH_2, 2 H), 1.33 (s, C(CH_3)$_3$, 18 H). Anal. Calcd (found) for $C_{19}H_{30}BBrN_2S_2Zn$: C, 45.0 (44.9); H, 5.97 (6.01); N, 5.53 (5.42).

[Ph(pz$^{t\mathrm{Bu}}$)Bt$^{t\mathrm{Bu}}$]Zn(CH$_3$). $Zn(CH_3)_2$ (0.3 mL, 0.6 mmol) was added to [Ph(pz$^{t\mathrm{Bu}}$)Bt$^{t\mathrm{Bu}}$]H (250 mg, 0.6 mmol) in 20 mL of toluene. The solution was stirred for 1 h, and then the solvent was removed under reduced pressure. The resulting white solid was washed with 15 mL of pentane and purified by recrystallization from CH_2Cl_2/Et_2O. Yield: 274 mg (92%). ^{1}H NMR ($CDCl_3$): δ 7.57 (d, (*o*-C_6H_5)B, 2 H), 7.37 (m, (*m*-C_6H_5)B and (*p*-C_6H_5)B, 3 H), 7.01 (s, 5-pz, 1 H), 6.00 (s, 4-pz, 1 H), 2.28 (s, BCH_2, 4 H), 1.47 (s, 3-pz-C(CH_3)$_3$, 9 H), 1.37 (s, SC(CH_3)$_3$, 18 H), −0.27 (s, Zn−CH_3, 3 H). Anal. Calcd (found) for $C_{24}H_{41}BN_2S_2Zn$: C, 57.9 (57.1); H, 8.30 (8.53); N, 5.63 (5.62).

[Ph(pz$^{t\mathrm{Bu}}$)Bt$^{t\mathrm{Bu}}$]Zn(SPh). Thiophenol (1.72 mL, 0.87 M in toluene, 1.5 mmol) was added to [Ph(pz$^{t\mathrm{Bu}}$)Bt$^{t\mathrm{Bu}}$]Zn(CH_3) (500 mg, 1 mmol) in 20 mL of CH_2Cl_2 at 0 °C. The solution was stirred for 1 h, and then the solvent was removed under reduced pressure. The resulting white solid was washed with 20 mL of pentane and purified by recrystallization from CH_2Cl_2/Et_2O. Yield: 520 mg (88%). ^{1}H NMR (CD_2Cl_2): δ 7.70 (d, (*o*-C_6H_5)S, 2 H), 7.55 (d, (*o*-C_6H_5)B, 2 H), 7.40 (m, (*m*-C_6H_5)B + (*p*-C_6H_5)B, 3 H), 7.25 (t, (*m*-C_6H_5)S, 2 H), 7.09 (m, (*p*-C_6H_5)S + 5-pz, 2 H), 6.08 (s, 4-pz, 1 H), 2.44 (d, BCH_2, 2 H), 2.23 (d, BCH_2, 2 H), 1.53 (s, 3-C(CH_3)$_3$, 9 H), 1.28 (s, SC(CH_3)$_3$, 18 H). Anal. Calcd (found) for $C_{29}H_{43}BN_2S_3Zn$: C, 58.8 (58.7); H, 7.32 (7.54); N, 4.73 (4.72).

{[PhTt$^{t\mathrm{Bu}}$]CdCl}$_2$. [PhTt$^{t\mathrm{Bu}}$]Tl (550 mg, 0.91 mmol) in 5 mL of CH_2Cl_2 was added to $CdCl_2$ (167 mg, 0.91 mmol) in 15 mL of Et_2O, yielding a clear solution and white solid. The solution was stirred for 2 h. After filtration the solvent was removed under reduced pressure,

(32) Wilker, J. J.; Lippard, S. J. *J. Am. Chem. Soc.* **1995**, *117*, 8682−8683.
(33) Vogel, A. T.; Cowan, D. M. *J. Chem. Soc.* **1943**, *21*, 16−24.
(34) Trofimenko, S.; Calabrese, J. C.; Thompson, J. S. *Inorg. Chem.* **1987**, *26*, 1507−1514.

yielding a light yellow solid. The solid was washed with (2 × 10 mL) portions of Et_2O to yield a white solid. Yield: 250 mg (51%). ^{1}H NMR ($CDCl_3$): δ 7.38 (d, *o*-C_6H_5, 2 H), 7.30 (t, *m*-C_6H_5, 2 H), 7.15 (t, *p*-C_6H_5, 1 H), 2.42 (br, BCH_2, 6 H), 1.50 (s, C(CH_3)$_3$, 27 H). Anal. Calcd (found) for $C_{42}H_{76}B_2Cd_2Cl_2S_6$: C, 46.2 (46.0); H, 7.02 (7.15).

Crystallographic Structural Determinations. Crystal, data collection, and refinement parameters are given in Table 1. For [PhTt$^{t\mathrm{Bu}}$]-ZnBr and [Ph(pz$^{t\mathrm{Bu}}$)Bt$^{t\mathrm{Bu}}$]Zn(SPh), the systematic absences in the diffraction data are uniquely consistent for the reported space group, and no evidence of symmetry higher than triclinic was observed in the diffraction data of {[PhTt$^{t\mathrm{Bu}}$]CdCl}$_2$ and [Ph(pz)Bt$^{t\mathrm{Bu}}$]ZnBr. *E*-Statistics and the value of *Z* suggested the centrosymmetric space group option, $P\bar{1}$, which yielded chemically reasonable and computationally stable results of refinement. The structures were solved using direct methods, completed by subsequent difference Fourier syntheses, and refined by full-matrix least-squares procedures. Empirical SADABS absorption corrections were applied to all data sets. The asymmetric unit of {[PhTt$^{t\mathrm{Bu}}$]CdCl}$_2$ contains half of the cadmium complex, which lies on an inversion center. All non-hydrogen atoms were refined with anisotropic displacement coefficients, and hydrogen atoms were treated as idealized contributions.

All software and sources of the scattering factors are contained in the SHELXTL (5.10) program library (G. Sheldrick, Siemens XRD, Madison, WI).

Acknowledgment. We gratefully acknowledge the financial support provided by the National Science Foundation (NYI and CHE-9974628 to C.G.R.) and the University of Delaware.

Supporting Information Available: Tables giving structure determination summary, atomic coordinates, bond lengths and bond angles, anisotropic thermal parameters, and hydrogen atom parameters for [PhTt$^{t\mathrm{Bu}}$]ZnBr, {[PhTt$^{t\mathrm{Bu}}$]CdCl}$_2$, [Ph(pz)Bt$^{t\mathrm{Bu}}$]ZnBr, and [Ph(pz$^{t\mathrm{Bu}}$)-Bt$^{t\mathrm{Bu}}$]Zn(SPh). This material is available free of charge via the Internet at http://pubs.acs.org.

IC000505Q